Quantum simulations of time travel can power nonclassical metrology

David R. M. Arvidsson-Shukur,[1] Aidan G. McConnell,[2] and Nicole Yunger Halpern[3, 4]

[1]*Hitachi Cambridge Laboratory, J. J. Thomson Avenue, Cambridge, CB3 0HE, United Kingdom*
[2]*Cavendish Laboratory, Department of Physics, University of Cambridge, Cambridge, CB3 0HE, United Kingdom*
[3]*Joint Center for Quantum Information and Computer Science,*
NIST and University of Maryland, College Park, MD 20742, USA
[4]*Institute for Physical Science and Technology, University of Maryland, College Park, MD 20742, USA*
(Dated: July 19, 2022)

Gambling agencies forbid late bets, placed after the winning horse crosses the finish line. A time-traveling gambler could cheat the system. We construct a gamble that one can win by simulating time travel with experimentally feasible entanglement manipulation. Our gamble echoes a common metrology protocol: A gambler must prepare probes to input into a metrology experiment. The goal is to infer as much information per probe as possible about a parameter's value. If the input is optimal, the information gained per probe can exceed any value achievable classically. The gambler chooses the input state analogously to choosing a horse. However, only after the probes are measured does the gambler learn which input would have been optimal. The gambler can "place a late bet" by effectively teleporting the optimal input back in time, via entanglement manipulation. Our Gedankenexperiment demonstrates that not only true time travel, but even a simulation offers a quantum advantage in metrology.

Introduction.—The arrow of time makes gamblers, investors, and quantum experimentalists perform actions that, in hindsight, are suboptimal. Examples arise in quantum metrology, the field of using nonclassical phenomena to estimate unknown parameters [1]. The optimal input states and final measurements are often known only once the experiment has finished [2]. Below, we present a Gedankenexperiment that circumvents this problem via quantum simulation of backward time travel.

A common metrological goal is to estimate the strength of a weak interaction between a system in a state $|\phi\rangle$ and a probe in a state $|\psi\rangle$. The interaction strength can be estimated from the data from several measured probes. Upon measuring probes at too high an intensity, detectors can saturate—cease to function until given time to reset. Reducing the number of probes measured is therefore often advantageous [3–9]. In such situations, one can utilize *weak-value amplification* to boost the rate of information obtained per measured probe [3–6, 10–12]. In weak-value amplification, the system is initialized in a state $|\phi_i\rangle$, the system interacts with the probe, and then the system is measured. If and only if the measurement outcome corresponds to $|\phi_f\rangle$, the probe is measured. Successful pre- and postselection guarantees that the probe carries a large quantity of information. Weak-value amplification stems from genuine nonclassicality, as reviewed below [13–15]. The nonclassicality originates in the postinteraction measurement, as well as the initialization, and so has sparked discussions about chronology-violating physics [16, 17].

Chronology-violating physics includes also *closed time-like curves* (CTCs) [18–24]. A CTC is a spacetime worldline that loops backward in time (Fig. 1). Particles that follow CTCs can travel backward in time with respect to chronology-respecting observers. Although allowed by general relativity, CTCs lead to logical para-
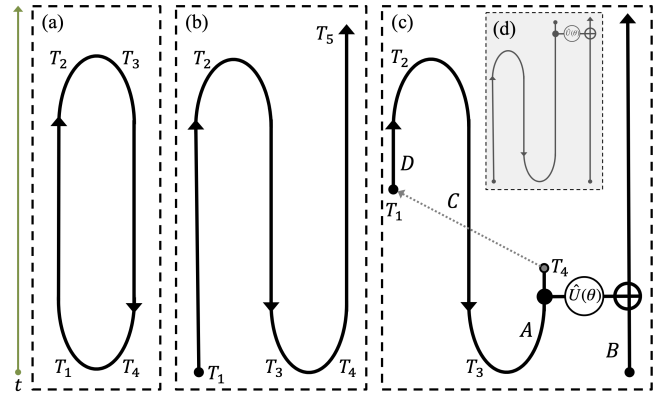

FIG. 1. Examples of chronology-violating particles traversing CTCs. ρ_{cv} denotes such particles' states. Time t, experienced by a chronology-respecting observer, runs from bottom to top. The time-traveling particle experiences time T. (a) Closed loop. (b) ρ_{cv} returns to its past and then travels forward in time again. (c) CTC interpretation of the successful trials of our Gedankenexperiment. ρ_{cv} is created at T_1 and travels forward in time until T_2. Then, it reverses temporal direction and travels backward in time until reaching T_3. After that, it again travels forward in time. ρ_{cv} then interacts with a chronology-respecting state, ρ_{cr}, and is subsequently destroyed, prior to ρ_{cv}'s creation (T_1). For comparison, the inset (d) depicts the standard teleportation, across space, of a quantum state needed as input for an interaction.

doxes. A famous example is the *grandfather paradox*: A time traveler travels back in time to kill her grandfather, before he fathers any children, such that the time traveler could never have been born... Such inconsistency characterizes classical CTCs. Two competing theories resolve such paradoxes, self-consistently reconciling general-relativistic CTCs with quantum theory [20–26]. We use the theory of *postselected CTCs* (PCTCs), motivated by the postselection in weak-value amplifica-

tion. Quantum states traversing PCTCs are equivalent to states undergoing postselected quantum circuits [23, 24].

In this work, we show that quantum simulations of PCTCs can effectively send useful states from the future to the past, providing access to nonclassical phenomena in quantum metrology. We propose a weak-value-amplification Gedankenexperiment for estimating the strength of an interaction between a system and a probe. The figure of merit, motivated by detector saturation, is the amount of information obtained per probe. As mentioned earlier, this rate can be nonclassically large if some probes are discarded conditionally on an earlier measurement of the system. But this information distillation requires that the system be initialized in a specific state. In our Gedankenexperiment, the optimal input state is unknown until after the system has been measured. We circumvent this challenge via quantum simulation of backward time travel: One can effectively teleport the optimal state from the experiment's end to its beginning. The simulated time travel sometimes fails, but at no detriment to the figure of merit, the amount of information gleaned from the remaining probes. These probes, retained only if the simulated time travel succeeds, carry amounts of information impossible to achieve classically. Thus, in weak-value amplification, the system can be initialized *after* the system–probe interaction—paradoxically, in chronology-respecting theories. Our conceptual results pinpoint a deep connection between quantum entanglement and retrocausal correlations that enable nonclassical advantages.

Background: Closed timelike curves.—Figure 1 shows examples of CTCs—spacetime wordlines that loop in the direction of time. There are two (main) theories of how to self-consistently describe CTCs quantum mechanically. The first theory is called Deutsch's CTCs (DCTCs) [20, 22]. DCTCs conserve a time traveler's state but not its correlations (entanglement) with chronology-respecting systems.

We use a second model: PCTCs [21–26]. Consider measuring a system that undergoes a PCTC. Whether the measurement happens before or after the PCTC does not affect the measurement statistics. Such self-consistency follows from modeling CTCs with quantum-teleportation circuits that involve postselection. The postselection ensures that time-traveling particles preserve their correlations with chronology-respecting systems.

Quantum circuits with entangled states can effectively realize PCTCs, as illustrated in Fig. 1. (The word "effectively" is used because one cannot empirically prove whether or not time travel *actually* happened [22].) ∪ depicts the creation of a Bell (maximally entangled) state [27], and ∩ depicts the future postselection onto that Bell state. In Fig. 1(a), the two entangled particles can be viewed as the forward-traveling (left) and backward-traveling (right) parts of one chronology-violating particle's worldline. The CTC in Fig. 1(b) can be simulated by a three-qubit quantum circuit for teleportation.

With probability 1/4, teleported qubits appear at the receiver's end, without the receiver's performing any local operation [28]. In these events, the teleported qubit was already at the receiver's end [21, 23].[1] Postselected on these outcomes, the circuit can be viewed as depicting one chronology-violating qubit's worldline. In the qubit's rest frame, the qubit is initialized at T_1. At T_2, it starts traveling backward according to the laboratory frame, until reaching the point of its "birth" at T_3. At T_4, the qubit reverses its temporal direction again, returning to traveling forward in time.

Below, we outline a Gedankenexperiment in which PCTCs can be used to achieve a nonclassical metrological advantage. But first, we introduce weak-value amplification in quantum metrology.

Weak-value amplification for metrology.—We now describe how to estimate the strength of a weak system–probe interaction. Weak-value amplification concentrates information, boosting the amount of information obtained per probe.

Using quantum metrology, one infers the value of an unknown parameter θ by measuring N copies of a state $|\Psi_\theta\rangle$ [1]. Every such procedure implies an estimator θ_e of θ. The Cramér-Rao inequality lower-bounds the precision of every unbiased θ_e:

$$\mathrm{Var}(\theta_e) \geq \frac{1}{N \cdot \mathcal{I}_q(\theta|\Psi_\theta)}. \tag{1}$$

$\mathcal{I}_q(\theta|\Psi_\theta)$ is the *quantum Fisher information*, which quantifies the average amount of information learned about θ per optimal measurement [29]. The quantum Fisher information has the form

$$\mathcal{I}_q(\theta|\Psi_\theta) = 4\langle\dot{\Psi}_\theta|\dot{\Psi}_\theta\rangle - 4|\langle\Psi_\theta|\dot{\Psi}_\theta\rangle|^2, \tag{2}$$

where $\dot{x} \equiv \partial x/\partial\theta$. For common estimators, Ineq. (1) is saturated when N is large. The larger $\mathcal{I}_q(\theta|\Psi_\theta)$ is, the more precisely one can estimate θ.

In this work, we consider estimating the strength of an interaction $\hat{U}(\theta) = e^{-i\theta\hat{\Pi}_a\otimes\hat{B}/2}$ between a system qubit in a state $|\phi\rangle_A$ and a probe qubit in a state $|\psi\rangle_B$. Here, $\theta \approx 0$ is the weak coupling strength, and $\hat{\Pi}_a \equiv |a\rangle\langle a|$ denotes a rank-1 projector on qubit A's Hilbert space. $\hat{B} \equiv |b^+\rangle\langle b^+| - |b^-\rangle\langle b^-|$ is a Hermitian operator acting on qubit B's Hilbert space, with eigenvalues ± 1. $\hat{U}(\theta)$ evolves $|\psi\rangle_B$ with a unitary evolution generated by $\hat{B}$, conditionally on qubit A's being in the state $|a\rangle$.

To measure the coupling strength θ, we prepare the system-and-probe state $|\Psi_0\rangle_{A,B} \equiv |\phi\rangle_A |\psi\rangle_B$, evolve it under $\hat{U}(\theta)$, and then measure the qubits. An information-optimal input is $|\Psi_0^\star\rangle_{A,B} = |a\rangle_A \frac{1}{\sqrt{2}}(|b^+\rangle_B +$

---

[1] A teleportation scheme that takes all possible outcomes into account, without the receiver's performing any local operations, transports an unknown qubit exactly as ineffectively as random guessing.

$|b^-\rangle_B)$; this state acquires the greatest possible quantum Fisher information, being maximally sensitive to changes in θ. The postinteraction state is

$$|\Psi^\star(\theta)\rangle_{A,B} \equiv \hat{U}(\theta) |\Psi_0^\star\rangle_{A,B}$$

$$= |a\rangle_A \frac{e^{-i\theta/2} |b^+\rangle_B + e^{i\theta/2} |b^-\rangle_B}{\sqrt{2}}. \quad (3)$$

According to Eq. (2), the average measurement yields $\mathcal{I}_q[\theta|\Psi_{A,B}^\star(\theta)] = 1$ unit of Fisher information per postinteraction state.

Usefully, one can distill much information into few probes. One measures system A and, conditionally on the outcome, discards or keeps (postselects) the probe B. Information distillation is particularly advantageous if one's detectors saturate. Then, qubit B merits measuring only if B carries much information [5, 7, 9]. We now review one such distillation scheme, *weak-value amplification* [3–6, 10–12].

One evolves $|\Psi_0^w\rangle_{A,B} \equiv |i\rangle_A \frac{1}{\sqrt{2}}(|b^+\rangle_B + |b^-\rangle_B)$ under $\hat{U}(\theta)$, then measures A in the basis $\{|f\rangle, |f^\perp\rangle\}$ [Fig. 2(a)]. If the outcome is $_A\langle f|$, B is measured. If not, B is destroyed. The postselected state is

$$|\Psi^{\mathrm{ps}}(\theta)\rangle_B = |\psi^{\mathrm{ps}}(\theta)\rangle_B / \sqrt{p_\theta^{\mathrm{ps}}}, \quad (4)$$

where $|\psi^{\mathrm{ps}}(\theta)\rangle_B \equiv (_A\langle f| \otimes \hat{1}_B) \hat{U}(\theta) |\Psi_0^w\rangle_{A,B}$. The probability of successful postselection is $p_\theta^{\mathrm{ps}} \equiv {}_B\langle\psi^{\mathrm{ps}}(\theta)|\psi^{\mathrm{ps}}(\theta)\rangle_B$. A little algebra simplifies the postselected state:

$$|\Psi^{\mathrm{ps}}(\theta)\rangle_B = \frac{e^{-i\theta_f \langle\hat{\Pi}_a\rangle_i/2} |b^+\rangle_B + e^{i\theta_f \langle\hat{\Pi}_a\rangle_i/2} |b^-\rangle_B}{\sqrt{2}}$$

$$+ \mathcal{O}(\theta^2), \quad (5)$$

if $|\theta \cdot_f \langle\hat{\Pi}_a\rangle_i| \ll 1$. The *weak value* of $\hat{\Pi}_a$ is $_f\langle\hat{\Pi}_a\rangle_i \equiv {}_A\langle f|\hat{\Pi}_a |i\rangle_A / {}_A\langle f|i\rangle_A$, the "expectation value" of $\hat{\Pi}_a$ preselected on the state $|i\rangle_A$ and postselected on $_A\langle f|$. The quantum Fisher information [Eq. (2)] of $|\Psi^{\mathrm{ps}}(\theta)\rangle_B$ is

$$\mathcal{I}_q[\theta|\Psi_B^{\mathrm{ps}}(\theta)] = \left|_f\langle\hat{\Pi}_a\rangle_i\right|^2 + \mathcal{O}(\theta). \quad (6)$$

Above, we found that the nonpostselected experiment's quantum Fisher information, $\mathcal{I}_q[\theta|\Psi_{A,B}(\theta)]$, has a maximum value of 1. The postselected experiment, however, can achieve a quantum Fisher information $\mathcal{I}_q[\theta|\Psi_B^{\mathrm{ps}}(\theta)] \gg 1$. Weak-value amplification does not increase the total amount of information gained from all the probes [30, 31], but distills large amounts of information into a few postselected probes.

Such anomalously large amounts of information witness nonclassical phenomena [7–9]. For small θ, Eq. (6) exceds 1 if, and only if, the weak value $|_f\langle\hat{\Pi}_a\rangle_i| > 1$, i.e., the weak value's magnitude exceeds the maximum eigenvalue of $\hat{\Pi}_a$. Such a weak value is called *anomalous*. Anomalous weak values arise from the quantum
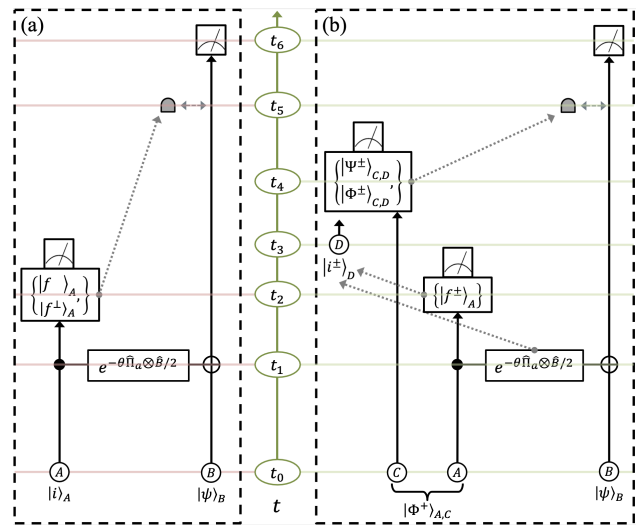

FIG. 2. Circuit diagrams for (a) standard and (b) PCTC-powered weak-value amplification. Time progresses in the laboratory's rest frame as one proceeds upward along the central, vertical axis. Black lines represent qubits. Dashed gray lines represent classical information.

resource *contextuality*: One can try to model quantum systems as being in real, but unknown, microstates like those in classical statistical mechanics. In such a framework, however, operationally indistinguishable quantum procedures cannot be modeled identically. This impossibility is contextuality [14, 15, 32, 33]. Contextuality is valuable. It enables weak-value amplification, which reduces the intensity of the probes impinging on saturable detectors, while endowing each detected probe with a large amount of information.

Metrological quantum advantage via PCTCs.— To perform weak-value amplification, an experimentalist needs to carefully set qubit A's input state, $|i\rangle_A$, and final measurement basis, $\{|f\rangle_A, |f^\perp\rangle_A\}$, such that $|_f\langle\hat{\Pi}_a\rangle_i| > 1$. Doing so requires knowledge of $\hat{\Pi}_a$. The goal is to simultaneously achieve a small weak-value denominator $_A\langle f|i\rangle_A$ and large numerator $_A\langle f|\hat{\Pi}_a|i\rangle_A$. If $\hat{\Pi}_a$ and the postselection basis are unknown, achieving the goal seems impossible.

We overcome this obstacle by combining PCTCs with postselected metrology. We assume that $\hat{\Pi}_a$ and the postselection basis $\{|f^\pm\rangle_A\}$ are unknown until just after (in the laboratory's rest frame) the interaction.[2] Can we nevertheless initialize $|\phi\rangle_A$ to take advantage of the contextuality? We answer affirmatively, by constructing a simulated PCTC.

Given a postselection outcome $_A\langle f^\pm|$, we choose the input state $|i^\pm\rangle_A$ such that $|_{f+}\langle\hat{\Pi}_a\rangle_{i+}| = |_{f-}\langle\hat{\Pi}_a\rangle_{i-}| \gg$

---

[2] These assumptions are unlikely to arise naturally in metrology but are needed in our Gedankenexperiment.

1.[3] As $\hat{\Pi}_a$ and $\{|f^{\pm}\rangle_A\}$ are known only after the interaction, we effectively create the input state $|\phi\rangle_A = |i^{\pm}\rangle_A$ after the interaction has taken place. Then, we simulate a PCTC to effectively teleport the state backward in time, such that $|\phi\rangle_A$ serves as an input in the interaction. Figure 2(b) illustrates our experiment with a quantum circuit.

In the laboratory's rest frame, our protocol proceeds as follows:

t_0: • A and C are entangled:

$$|\Phi^+\rangle_{A,C} = \frac{1}{\sqrt{2}}\left(|0\rangle_A|0\rangle_C + |1\rangle_A|1\rangle_C\right).$$

• Qubit B is initialized as

$$|\Psi\rangle_B = \frac{1}{\sqrt{2}}\left(|b^+\rangle_B + |b^-\rangle_B\right).$$

t_1: • A and B interact via $\hat{U}(\theta) = e^{-i\theta\hat{\Pi}_a \otimes \hat{B}/2}$. The value of θ and the form of $\hat{\Pi}_a = |a\rangle\langle a|$ are unknown.

t_2: • The as-yet-unknown, optimal measurement basis $\{|f^{\pm}\rangle_A\}$ is revealed.

• A is measured in this basis.

t_3: • Information about $\hat{\Pi}_a$ and about the outcome $_A\langle f^{\pm}|$ reaches D.

• Qubit D is created and initialized in $|i^{\pm}\rangle_D$.

t_4: • C and D are measured in the Bell basis [27].

• Outcome $_{C,D}\langle\Phi^+|$ effectively teleports $|i^{\pm}\rangle_D$ to the time-t_0 system A.[4]

t_5: • If and only if outcome $_{C,D}\langle\Phi^+|$ was obtained at t_4, a beam blocker is removed from B's path.

t_6: • If the beam blocker was removed, B is measured in the $\left\{\frac{1}{\sqrt{2}}(|b^+\rangle \pm |b^-\rangle)\right\}$ basis.

The supplementary material presents the mathematical details behind our protocol's effectiveness.

Repeated experiments that involve final B measurements produce an anomalously large weak value. It amplifies the quantum Fisher information about θ to nonclassically large values. We have thus shown that, in weak-value amplification, the preselected system state can effectively be created *after* the interaction—even after the state has been measured and destroyed. This

---

[3] In general, $\langle i^-|i^+\rangle \neq 0$.
[4] This postselection is onto a copy of the state prepared initially, $|\Phi^+\rangle$. Therefore, our circuit preserves correlations (between chronology-violating and chronology-respecting systems) as required by the definition of PCTCs.

point is visible in Fig. 1(c), a CTC diagram of our protocol. The inset [Fig. 1(d)] depicts the standard teleportation, across space, of a quantum state to be inputted into an interaction. The state's initialization is postponed, and the state's destruction is advanced, in Fig. 1(c). These changes do not affect the chronology-respecting state's final form.

One could imagine three objections. First, some postselections—and so teleportation attempts—fail. However, these failures do not lower the figure of merit, the amount of information in the probes that pass the blocker. As further reassurance: Our setup does not allow classical information to be sent to the past. The improved information-per-detection rate is available only at the end of the experiment.

Second, our assumption about when the information needed to choose $|i^{\pm}\rangle$ arrives may seem artificial. It is. However, in most realistic metrology experiments, the optimal strategy remains unknown until after the experiment [2]. Furthermore, our study's purpose is foundational—to demonstrate the power of quantum-simulating PCTCs to achieve a quantum advantage.

Third, one might view our experiment as involving a preselected state $|\Phi^+\rangle_{C,A}|i^{\pm}\rangle_D$ and a postselected state $_A\langle f^{\pm}|_{D,C}\langle\Phi^+|$. Our experiment would show no more retrocausality than earlier experiments with pre- and postselection. However, such an interpretation contradicts the definitions of pre- and postselection, as D is created after A is postselected.

The limit as $\theta \to 0$ implies more counterintuitive phenomena. First, B and the rest of the system always remain in a tensor-product bipartite state—share no correlations, let alone entanglement. Yet the quantum Fisher information of B can still be nonclassically large. Furthermore, imagine, in addition to the $\theta \to 0$ limit, measuring B between t_1 and t_2, before any other measurement and before D is initialized. At time t_5, one would postprocess the data from the B measurements. One would uncover the same contextuality as in conventional weak-value amplification [Fig. 2(a)]. This conclusion paradoxically holds even though B is destroyed before A, C, and D are measured. How? If PCTCs are real (perhaps probabilistic) effects of quantum mechanics, the nonclassicality comes from time travel. Without real PCTCs, the paradox's resolution depends on entanglement

For comparison: Previous works have addressed the advantages offered by CTCs [23, 34–42]. For example, PCTCs would boost a computer's computational power [23, 34–36, 38]. (Also classical computers can achieve such computational power if postselected.) Our metrological protocol differs, posing a paradox even in the absence of true CTCs: Probabilistically simulating PCTCs suffices for achieving the nonclassical advantage. Relatedly, Svetlichny shows that PCTC simulation can effect a Bell measurement of a state before the state is created [22]. Also, probabilistically simulating DCTCs enables nonorthogonal-state discrimination [43]. However,

our result differs from these two by entailing that CTC simulation can enable a truly nonclassical advantage—one sourced by contextuality—in the past.

Conclusions.—We have shown how simulating time travel with entanglement benefits the estimation of a coupling strength. A certain "key" input state is needed to unlock a quantum advantage. However, in our setup, the ideal input state is known only after the interaction takes place and the system is measured. We have shown how simulating quantum time travel allows for the key to be created at a later time and then effectively teleported back in time to serve as the experiment's input. The time travel can be simulated with postselected quantum-teleportation circuits. Our Gedankenexperiment thus draws an metrological advantage from apparently retro-causal correlations creatable with quantum circuits and entangled states. While PCTCs do not allow you to go back and alter your past, they do allow you to create a better tomorrow by fixing yesterday's problems today.

[1] V. Giovannetti, S. Lloyd, and L. Maccone, Nature photonics **5**, 222 (2011).

[2] W. Salmon, S. Strelchuk, and D. Arvidsson-Shukur, (2022), 10.48550/ARXIV.2205.14142.

[3] J. Dressel, M. Malik, F. M. Miatto, A. N. Jordan, and R. W. Boyd, Rev. Mod. Phys. **86**, 307 (2014).

[4] S. Pang, J. Dressel, and T. A. Brun, Phys. Rev. Lett. **113**, 030401 (2014).

[5] J. Harris, R. W. Boyd, and J. S. Lundeen, Phys. Rev. Lett. **118**, 070802 (2017).

[6] L. Xu, Z. Liu, A. Datta, G. C. Knee, J. S. Lundeen, Y.-q. Lu, and L. Zhang, Phys. Rev. Lett. **125**, 080501 (2020).

[7] D. R. M. Arvidsson-Shukur, N. Yunger Halpern, H. V. Lepage, A. A. Lasek, C. H. W. Barnes, and S. Lloyd, Nature Communications **11**, 3775 (2020).

[8] J. H. Jenne and D. R. M. Arvidsson-Shukur, (2021), 10.48550/ARXIV.2104.09520.

[9] N. Lupu-Gladstein, Y. B. Yilmaz, D. R. M. Arvidsson-Shukur, A. Brodutch, A. O. T. Pang, A. M. Steinberg, and N. Y. Halpern, Phys. Rev. Lett. **128**, 220504 (2022).

[10] Y. Aharonov, D. Z. Albert, and L. Vaidman, Phys. Rev. Lett. **60**, 1351 (1988).

[11] I. M. Duck, P. M. Stevenson, and E. C. G. Sudarshan, Phys. Rev. D **40**, 2112 (1989).

[12] O. Hosten and P. Kwiat, Science **319**, 787 (2008).

[13] J. Tollaksen, J. Phys. A **40**, 9033 (2007).

[14] M. F. Pusey, Phys. Rev. Lett. **113**, 200401 (2014).

[15] R. Kunjwal, M. Lostaglio, and M. F. Pusey, Phys. Rev. A **100**, 042116 (2019).

[16] Y. Aharonov and L. Vaidman, *Time in quantum mechanics* (Springer, 2008) pp. 399–447.

[17] M. S. Leifer and M. F. Pusey, Proceedings of the Royal Society A: Mathematical, Physical and Engineering Sciences **473**, 20160607 (2017).

[18] K. Gödel, Rev. Mod. Phys. **21**, 447 (1949).

[19] M. S. Morris, K. S. Thorne, and U. Yurtsever, Phys. Rev. Lett. **61**, 1446 (1988).

[20] D. Deutsch, Physical Review D **44**, 3197 (1991).

[21] C. H. Bennett, in *Proceedings of QUPON* (Wien, 2005).

[22] G. Svetlichny, International Journal of Theoretical Physics **50**, 3903 (2011).

[23] S. Lloyd, L. Maccone, R. Garcia-Patron, V. Giovannetti, Y. Shikano, S. Pirandola, L. A. Rozema, A. Darabi, Y. Soudagar, L. K. Shalm, and A. M. Steinberg, Phys. Rev. Lett. **106**, 040403 (2011).

[24] S. Lloyd, L. Maccone, R. Garcia-Patron, V. Giovannetti, and Y. Shikano, Phys. Rev. D **84**, 025007 (2011).

[25] J.-M. A. Allen, Phys. Rev. A **90**, 042107 (2014).

[26] T. A. Brun and M. M. Wilde, Foundations of Physics **47**, 375 (2017).

[27] M. A. Nielsen and I. L. Chuang, *Quantum Computation and Quantum Information: 10th Anniversary Edition*, 10th ed. (Cambridge University Press, New York, NY, USA, 2011).

[28] C. H. Bennett, G. Brassard, C. Crépeau, R. Jozsa, A. Peres, and W. K. Wootters, Phys. Rev. Lett. **70**, 1895 (1993).

[29] S. L. Braunstein and C. M. Caves, Phys. Rev. Lett. **72**, 3439 (1994).

[30] J. Combes, C. Ferrie, Z. Jiang, and C. M. Caves, Phys. Rev. A **89**, 052117 (2014).

[31] C. Ferrie and J. Combes, Phys. Rev. Lett. **112**, 040406 (2014).

[32] R. W. Spekkens, Phys. Rev. A **71**, 052108 (2005).

[33] M. Lostaglio, arXiv preprint arXiv:2004.01213 (2020).

[34] T. A. Brun, Foundations of Physics Letters **16**, 245 (2003).

[35] S. Aaronson, (2004), 10.48550/ARXIV.QUANT-PH/0412187.

[36] S. Aaronson and J. Watrous, Proceedings of the Royal Society A: Mathematical, Physical and Engineering Sciences **465**, 631 (2009).

[37] T. A. Brun, J. Harrington, and M. M. Wilde, Phys. Rev. Lett. **102**, 210402 (2009).

[38] T. A. Brun and M. M. Wilde, Foundations of Physics **42**, 341 (2012).

[39] T. A. Brun, M. M. Wilde, and A. Winter, Phys. Rev. Lett. **111**, 190401 (2013).

[40] J. L. Pienaar, T. C. Ralph, and C. R. Myers, Phys. Rev. Lett. **110**, 060501 (2013).

[41] J. Bub and A. Stairs, Phys. Rev. A **89**, 022311 (2014).

[42] M. Bartkiewicz, A. Grudka, R. Horodecki, J. Łodyga, and J. Wychowaniec, Phys. Rev. A **99**, 022304 (2019).

[43] C. Vairogs, V. Katariya, and M. M. Wilde, Phys. Rev. A **105**, 052434 (2022).

Appendix A: Figures 2(a) and (b) prepare the same postselected B state

Here, we show that the postselected final state of B in Fig. 2(a) equals that in Fig. 2(b). In the main text, we showed that the postselected final state of B in Fig. 2(a) is [Eq. (4)]

$$|\Psi^{\mathrm{ps}}(\theta)\rangle_B = \frac{1}{\sqrt{p_\theta^{\mathrm{ps}}}} |\psi^{\mathrm{ps}}(\theta)\rangle_B \tag{A1}$$

$$\equiv \frac{1}{\sqrt{p_\theta^{\mathrm{ps}}}} \left(_A \langle f| \otimes \hat{1}_B\right) e^{-i\theta\hat{\Pi}_a \otimes \hat{B}/2} |i\rangle_A |\psi\rangle_B, \tag{A2}$$

where $p_\theta^{\mathrm{ps}} \equiv {}_B \langle \psi^{\mathrm{ps}}(\theta)|\psi^{\mathrm{ps}}(\theta)\rangle_B$ and $|\psi\rangle_B \equiv \frac{1}{\sqrt{2}}(|b^+\rangle_B + |b^-\rangle_B)$

We now calculate how the whole-system state evolves throughout our protocol, as described in the main text and Fig. 2(b). Immediately after t_0, the joint state is

$$|\Psi(t_0)\rangle_{A,B,C} \equiv \frac{1}{\sqrt{2}} \left(|0\rangle_A |0\rangle_C + |1\rangle_A |1\rangle_C\right) |\psi\rangle_B. \tag{A3}$$

Immediately after t_1, the joint state is

$$|\Psi_\theta(t_1)\rangle_{A,B,C} \equiv \left(e^{-i\theta\hat{\Pi}_a \otimes \hat{B}/2} \otimes \hat{1}_C\right) |\Psi(t_0)\rangle_{A,B,C}. \tag{A4}$$

Immediately after t_2, qubit A is measured, yielding an outcome $_A \langle f^\pm|$. The joint state is

$$|\Psi_\theta(t_2)\rangle_{B,C} \equiv \frac{1}{\sqrt{N_2}} \left(_A \langle f^\pm| \otimes \hat{1}_{B,C}\right) \left(e^{-i\theta\hat{\Pi}_a \otimes \hat{B}/2} \otimes \hat{1}_C\right) |\Psi(t_0)\rangle_{A,B,C}. \tag{A5}$$

N_2 is a normalization factor. Immediately after t_3, the joint state is

$$|\Psi_\theta(t_3)\rangle_{B,C,D} \equiv |\Psi_\theta(t_2)\rangle_{B,C} |i^\pm\rangle_D \tag{A6}$$

$$= \frac{1}{\sqrt{N_2}} \left(_A \langle f^\pm| \otimes \hat{1}_{B,C,D}\right) \left(e^{-i\theta\hat{\Pi}_a \otimes \hat{B}/2} \otimes \hat{1}_{C,D}\right) |\Psi(t_0)\rangle_{A,B,C} |i^\pm\rangle_D. \tag{A7}$$

At t_4 qubits C and D are measured in the Bell basis, $\left\{|\Psi^\pm\rangle = \frac{1}{\sqrt{2}}\left(|0\rangle|1\rangle \pm |1\rangle|0\rangle\right), |\Phi^\pm\rangle = \frac{1}{\sqrt{2}}\left(|0\rangle|0\rangle \pm |1\rangle|1\rangle\right)\right\}$. At t_5, B is discarded unless the Bell measurement yielded outcome $_{C,D} \langle \Phi^+|$. Immediately after t_5, the state is

$$|\Psi_\theta(t_5)\rangle_B \equiv \frac{1}{\sqrt{N_5}} \left(\hat{1}_B \otimes {}_{C,D} \langle \Phi^+|\right) |\Psi(t_3)\rangle_{B,C,D} \tag{A8}$$

$$= \frac{1}{\sqrt{N_5}} \left(_A \langle f^\pm| \otimes \hat{1}_B \otimes {}_{C,D} \langle \Phi^+|\right) \left(e^{-i\theta\hat{\Pi}_a \otimes \hat{B}/2} \otimes \hat{1}_{C,D}\right) |\Psi(t_0)\rangle_{A,B,C} |i^\pm\rangle_D \tag{A9}$$

$$= \frac{1}{\sqrt{N_5}} \left(_A \langle f^\pm| \otimes \hat{1}_B \otimes {}_{C,D} \langle \Phi^+|\right) \left(e^{-i\theta\hat{\Pi}_a \otimes \hat{B}/2} \otimes \hat{1}_{C,D}\right) \frac{1}{\sqrt{2}} \left(|0\rangle_A |0\rangle_C + |1\rangle_A |1\rangle_C\right) |\psi\rangle_B |i^\pm\rangle_D. \tag{A10}$$

N_5 is a normalization factor. We can expand the factor $|\Phi^+\rangle_{A,C} |i^\pm\rangle$ in the Bell basis for C and D:

$$|\Psi_\theta(t_5)\rangle_B = \frac{1}{\sqrt{N_5}} \left(_A \langle f^\pm| \otimes \hat{1}_B \otimes {}_{C,D} \langle \Phi^+|\right) \left(e^{-i\theta\hat{\Pi}_a \otimes \hat{B}/2} \otimes \hat{1}_{C,D}\right) |\psi\rangle_B$$

$$\times \frac{1}{2} \left[|\Phi^+\rangle_{C,D} |i^\pm\rangle_A + |\Phi^-\rangle_{C,D} \hat{Z}_A |i^\pm\rangle_A + |\Psi^+\rangle_{C,D} \hat{X}_A |i^\pm\rangle_A + |\Psi^-\rangle_{C,D} \hat{X}_A \hat{Z}_A |i^\pm\rangle_A\right]. \tag{A11}$$

$\hat{X}$ and $\hat{Z}$ denote Pauli matrices. We simplify the above expression by calculating the inner product with $_{C,D} \langle \Phi^+|$:

$$|\Psi_\theta(t_5)\rangle_B = \frac{1}{\sqrt{N_5}} \left(_A \langle f^\pm| \otimes \hat{1}_B\right) \left(e^{-i\theta\hat{\Pi}_a \otimes \hat{B}/2}\right) |i^\pm\rangle_A |\psi\rangle_B. \tag{A12}$$

Choosing the optimal system preparation $|\psi\rangle_B = \frac{1}{\sqrt{2}}(|b^+\rangle_B + |b^-\rangle_B)$ yields $N_5 = p_\theta^{\mathrm{ps}}$. Consequently, $|\Psi_\theta(t_5)\rangle_B = |\Psi^{\mathrm{ps}}(\theta)\rangle_B$, and the circuits preparing the postselected states in Figs. 2(a) and 2(b) are equivalent.